catalysts

Article

Dimethyl-Aluminium Complexes Bearing Naphthyl-Substituted Pyridine-Alkylamides as Pro-Initiators for the Efficient ROP of ε-Caprolactone

Andrew P. Armitage [1], Olivier Boyron [2], Yohan D. M. Champouret [1], Mehzabin Patel [1], Kuldip Singh [1] and Gregory A. Solan [1,*]

[1] Department of Chemistry, University of Leicester, University Road, Leicester LE1 7RH, UK;
E-Mails: armita@matthey.com (A.P.A.); champouy@hotmail.com (Y.D.M.C.);
mehzabin49@hotmail.com (M.P.); ks42@leicester.ac.uk (K.S.)

[2] Laboratoire de Chimie, Catalyse, Polymères et Procédés, Université de Lyon, CNRS-UCBL,
43 Boulevard du 11 Novembre 1918, Villeurbanne 69616, France;
E-Mail: olivier.boyron@univ-lyon1.fr

* Author to whom the correspondence should be addressed: E-Mail: gas8@leicester.ac.uk;
Tel.: +44-116-252-2096; Fax: +44-116-252-3789.

Abstract: Three sterically-enhanced 2-imino-6-(1-naphthyl)pyridines, 2-{CMe=N(Ar)}-6-(1-$C_{10}H_7$)C_5H_3N [Ar = 2,6-*i*-$Pr_2C_6H_3$ (**L1**$_{dipp}$), 2,4,6-*i*-$Pr_3C_6H_2$ (**L1**$_{tripp}$), 4-Br-2,6-*i*-$Pr_2C_6H_2$ (**L1**$_{Brdipp}$)], differing only in the electronic properties of the *N*-aryl group, have been prepared in high yield by the condensation reaction of 2-{CMe=O}-6-(1-$C_{10}H_7$)C_5H_3N with the corresponding aniline. Treatment of **L1**$_{dipp}$, **L1**$_{tripp}$ and **L1**$_{Brdipp}$ with two equivalents of AlMe₃ at elevated temperature affords the distorted tetrahedral 2-(amido-prop-2-yl)-6-(1-naphthyl)pyridine aluminum dimethyl complexes, [2-{CMe₂N(Ar)}-6-(1-$C_{10}H_7$)C_5H_3N]AlMe₂ [Ar = 2,6-*i*-$Pr_2C_6H_3$ (**1a**), 2,4,6-*i*-$Pr_3C_6H_2$ (**1b**), 4-Br-2,6-*i*-$Pr_2C_6H_2$ (**1c**)], in good yield. The X-ray structures of **1a**–**1c** reveal that complexation has resulted in concomitant C–C bond formation via methyl migration from aluminum to the corresponding imino carbon in **L1**$_{aryl}$; in solution, the restricted rotation of the pendant naphthyl group in **1** confers inequivalent methyl ligand environments. The ring opening polymerization of ε-caprolactone employing **1**, in the presence of benzyl alcohol, proceeded efficiently at 30 °C producing polymers of narrow molecular weight distribution with the catalytic activities dependent on the nature of the substituent located at the

4-position of the *N*-aryl group with the most electron donating *i*-Pr derivative exhibiting the highest activity (**1b** > **1a** > **1c**); at 50 °C **1b** mediates 100% conversion of the monomer to polycaprolactone (poly(CL)) in one hour. In addition to **1a**, **1b** and **1c**, the single crystal X-ray structures are reported for **L1**dipp and **L1**tripp.

Keywords: aluminum; naphthyl-substituted *N,N*-pyridine-alkylamide; ring opening polymerization; ε-caprolactone; electronic effect

1. Introduction

The controlled ring-opening polymerization (ROP) of cyclic esters to give biodegradable polymers (e.g., poly (lactic acid), poly (caprolactone)) mediated by well-defined organo-aluminum (III) precursors and their alkoxide derivatives has been the subject of extensive research over the last two decades, or so [1–5]. As the catalytic properties of the aluminum species employed are greatly influenced by the ancillary ligand (both electronically and sterically), a wide variety of multidentate ligand architectures have been developed and investigated in this field. While early reports focused on dianionic tetradentate ligands [6–20], more recent studies have highlighted the considerable potential of using tridentate [21–29] and bidentate [20,30–42] ligand sets as monoanionic ancillaries for potent and well-behaved AlR₂-based (R = alkyl) pro-initiators.

We have been attracted by the intriguing properties displayed by pyridylimine-containing ligands including their redox activity [43,44] and their capacity to undergo nucleophilic attack on the imine carbon [45–50] and the pyridine ring [51]. Indeed, the thermally-induced migration of an Al-alkyl to the imino carbon of a coordinated *N,N*-pyridylimine represents a powerful tool for transforming a pyridylimine into a pyridyl-alkylamide (and pyridyl-alkylamine on hydrolysis [45,52]). Moreover, functionalizing the 6-position of the pyridine moiety of the pyridylimine with an aryl or 1-naphthyl group presents a versatile set of substrates for studying *ortho vs. peri*-palladation reactions during the formation of *N,N,C*-chelates [53,54]. Likewise, *N,N*-pyridyl-alkylamides and their 6-aryl and -naphthyl derivatives have also been attracting attention due, in large measure, to their emergence as supports for exceptionally active *N,N*- [45,55,56] and *N,N,C*-bound group 4 olefin polymerization catalysts [57–60].

In this article we are concerned with exploiting the reactivity of the imino unit in a series of sterically-hindered 6-naphthyl-substituted pyridyl-ketimines, **L1** (R = H, *i*-Pr, Br; see Figure 1), towards nucleophilic attack with a view to forming aluminum methyl complexes bound by a series of electronically distinct pyridyl-alkylamides, **L2** (R = H, *i*-Pr, Br). The potential of the naphthyl group to undergo *peri/ortho* C–H sp²-activation during complexation or simply provide a bulky substituent with restricted mobility, presents a further point of interest. The resultant aluminum methyl complexes will be screened, in the presence of benzyl alcohol, for the ROP of ε-CL and any electronic effect imparted by the 4-R-substituted *N*-aryl group on the catalytic performance, investigated.
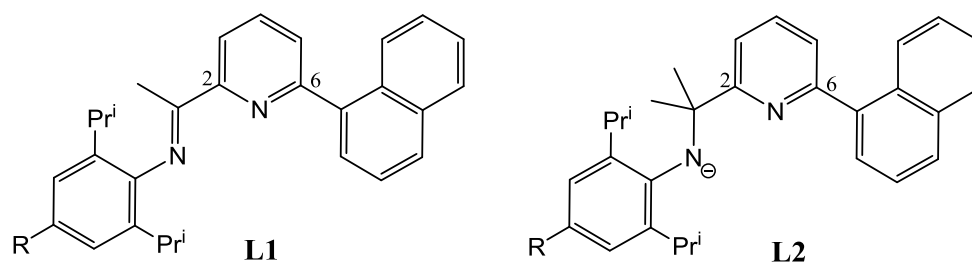
Figure 1. 2-Imino-6-(1-naphthyl)pyridine (**L1**) and monoanionic 2-(amido-prop-2-yl)-6-(1-naphthyl)pyridine (**L2**).

2. Results and Discussion

2.1. Synthetic and Structural Aspects

The 2-imino-6-(1-naphthyl)pyridines, $2\text{-}\{CMe=N(Ar)\}\text{-}6\text{-}(1\text{-}C_{10}H_7)C_5H_3N$ [Ar = $2,6\text{-}i\text{-}Pr_2C_6H_3$ (**L1**dipp), $2,4,6\text{-}i\text{-}Pr_3C_6H_2$ (**L1**tripp), $4\text{-}Br\text{-}2,6\text{-}i\text{-}Pr_2C_6H_2$ (**L1**Brdipp)], have been prepared as pale yellow to green solids in high yield by the condensation reaction of $2\text{-}\{CMe=O\}\text{-}6\text{-}(1\text{-}C_{10}H_7)C_5H_3N$ with the corresponding aniline (Scheme 1). The precursor ketone is not commercially available and has been synthesized using a variation of the previously reported Suzuki cross-coupling reaction of 1-naphthyl boronic acid with 2-bromo-6-acetylpyridine [61]. Compound **L1**dipp has been reported before [53,62], although no characterization data were disclosed. Hence, **L1**dipp and its substituted counterparts, **L1**tripp and **L1**Brdipp, have been characterized by a combination of ^1H, ^{13}C $\{^1H\}$ NMR, IR spectroscopy and mass spectrometry (see Experimental Section).
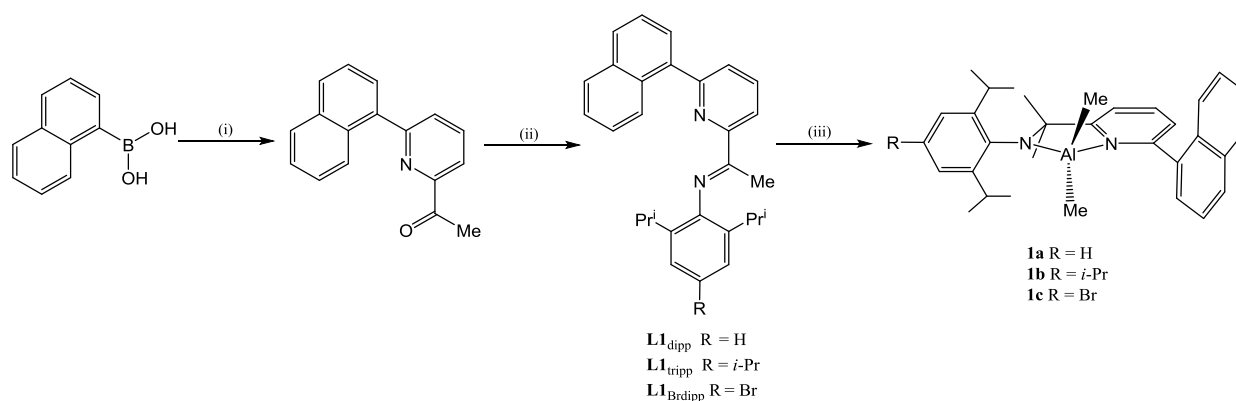
Scheme 1. Reagents and conditions: (i) $2\text{-}Br\text{-}6\text{-}(CMeO)\text{-}C_5H_3N$, cat. $Pd(PPh_3)_4$, K_2CO_3 (aq), toluene-EtOH, heat; (ii) $4\text{-}R\text{-}2,6\text{-}i\text{-}Pr_2C_6H_2NH_2$, cat. H^+, MeOH, heat; (iii) 2 AlMe₃, toluene, heat.

In addition, single-crystal X-ray diffraction studies have been performed on **L1**dipp and **L1**tripp. Typically, crystals suitable for the structural determinations were grown by slow evaporation of methanol solutions of the compound. A view of **L1**tripp is depicted in Figure 2 (see also Figures S1 and S2); selected bond distances and angles are listed for both **L1**dipp and **L1**tripp in Table 1. The structures are similar with a central pyridine ring substituted at its 6-position by a 1-naphthyl group and at the 2-position by an imine unit [C(6)–N(2) 1.282(3) Å (**L1**dipp), 1.280(5) Å (**L1**tripp)]. The

pyridine nitrogen adopts a *trans* configuration with respect to the neighboring imine nitrogen [tors.: N(1)–C(5)–C(6)–N(2) 174.3° (**L1**$_{dipp}$), 170.9° (**L1**$_{tripp}$)], while the 1-napthyl group undergoes some tilting with respect to the neighboring pyridine [tors.: C(32)–C(23)–C(1)–N(1) 48.5° (**L1**$_{dipp}$), 38.2° (**L1**$_{tripp}$)], in a manner similar to that found in related 1-naphthyl-substituted pyridines [63,64]. For both structures the 2,6-diisopropylphenyl rings are inclined essentially orthogonally [C(6)–N(2)–C(13)–C(12) 82.0° (**L1**$_{dipp}$), 88.6° (**L1**$_{tripp}$)] to the adjacent pyridylimine plane.
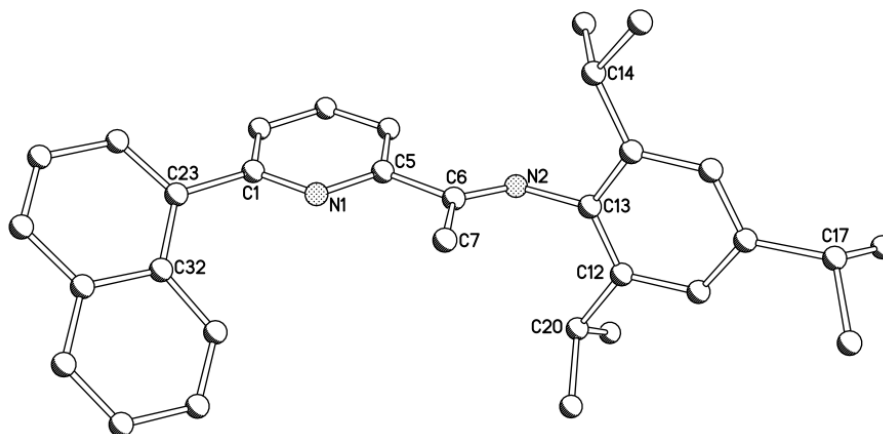

Figure 2. Molecular structure of **L1**$_{tripp}$ with atom labeling scheme; all hydrogen atoms have been omitted for clarity.

Table 1. Selected bond distances (Å) and angles (deg) for **L1**$_{dipp}$ and **L1**$_{tripp}$.

Compound	Bond Distances (Å)					Bond Angles (deg)	
	C(6)–N(2)	C(6)–C(7)	C(1)–C(23)	C(5)–C(6)	N(2)–C(13)	C(6)–N(2)–C(13)	C(7)–C(6)–N(2)
L1$_{dipp}$	1.282(3)	1.496(4)	1.503(3)	1.488(4)	1.419(3)	120.6(2)	125.8(2)
L1$_{tripp}$	1.280(5)	1.488(6)	1.482(6)	1.502(5)	1.430(5)	121.2(4)	126.5(4)

Compounds **L1**$_{dipp}$, **L1**$_{tripp}$ and **L1**$_{Brdipp}$ all display peaks corresponding to the protonated molecular ions in their ESI mass spectra while their IR spectra reveal characteristic ν(CN)$_{imine}$ bands *ca.* 1642 cm^{-1}. Further support for imine formation is provided by the ^{1}H NMR spectra which show signals for the ketimine methyl protons at *ca.* δ 2.2 (**L1**$_{dipp}$–**L1**$_{Brdipp}$) (see Figures S3–S5); the imino carbons are seen at *ca.* δ 160 in their ^{13}C{^{1}H} NMR spectra (see Figures S6–S8).

Reaction of ketimine-containing **L1**$_{dipp}$–**L1**$_{Brdipp}$ with two equivalents of trimethylaluminum in toluene at refluxing temperatures overnight results in complexation and methylation of the ketimine carbon moiety to afford the air sensitive 2-(amido-prop-2-yl)-6-(1-naphthyl)pyridine aluminum dimethyl complexes, [2-{CMe$_2$N(Ar)}-6-(1-C$_{10}$H$_7$)C$_5$H$_3$N]AlMe$_2$ [Ar = 2,6-*i*-Pr$_2$C$_6$H$_3$ (**1a**), 2,4,6-*i*-Pr$_3$C$_6$H$_2$ (**1b**), 4-Br-2,6-*i*-Pr$_2$C$_6$H$_2$ (**1c**)], in good yield (Scheme 1). Leaving the reaction longer at the same temperature or increasing the ratio of trimethylaluminum gave no evidence for an *ortho*- nor *peri*- C-H activated naphthyl species [53]. Complexes **1** have been both characterized by NMR and IR spectroscopy, mass spectrometry and gave satisfactory microanalytical data (see Experimental section). In addition, single-crystal X-ray diffraction studies were performed on **1a–1c**.

Single crystals of **1a**, **1b**, and **1c** suitable for X-ray determination were grown by slow cooling of acetonitrile solutions of each complex that had been previously brought to reflux. A perspective view

of representative **1c** is shown in Figure 3 (see also Figures S9–S11); selected bond distances and angles for all three structures are collected in Table 2. In each structure an aluminum center is bound by a monoanionic *N,N*-pyridine-alkylamide chelate along with two methyl ligands to complete a distorted tetrahedral geometry. The bite angle for the bidentate ligand ranges from 83.9(2)° up to 85.4(2)°, while the X–M–X angles between monodentate methyl ligands are closer to tetrahedral, ranging from 111.1(3)° up to 113.5(3)°. The presence of the *gem*-dimethyl group within the bidentate ligand backbone in **1a**, **1b** and **1c** confirms the successful methyl migration to the imine unit in **L1**aryl and an associated elongation of the C(8)–N(2) bond by *ca.* 0.2 Å is observed. The five-membered chelate rings display some variation in the degree of puckering between structures which is best exemplified by the C(7)–C(8)–N(2)–Al(1) torsion angles that vary between 1.3° (**1b**) and 27.1° (**1c**). Of the two Al–N bonds present in each structure, the one involving the amide [N(2)] is the shorter consistent with the ionic contribution to the bonding; no clear effects caused by the change in *N*-aryl 4-R group on the Al–N(2)amide distances are apparent between structures. In comparison with **L1**dipp/tripp the pendant naphthyl groups in **1a**–**1c** are tilted more towards orthogonality with respect to the adjacent pyridine unit [tors.: N(1)–C(3)–C(23)–C(32) 75.3° (**1a**), 69.5° (**1b**), 65.5° (**1c**)], with the result that one of the two Al–Me groups faces the fused diarene unit. Similar alkyl migration reactions mediated by alkylaluminums have been reported elsewhere [45–52], and indeed computational studies suggest a radical pathway for the transformation [44]. The closest comparators to **1** are [2-{CMe2N(2,6-*i*-Pr2C6H3)}-6-(R)C5H3N]AlMe2 (R = *i*-Pr, *t*-Bu) which display similar bond parameters [45].

Table 2. Selected bond distances (Å) and angles (°) for **1a**, **1b** and **1c**.

Complex	Bond Distances (Å)							
	Al(1)–C(1)	Al(1)–C(2)	Al(1)–N(1)	Al(1)–N(2)	C(8)–N(2)	C(3)–C(23)	C(11)–N(2)	C(14)–R
1a	1.950(2)	1.990(2)	2.003(2)	1.838(2)	1.471(3)	1.490(3)	1.429(3)	-
1b	1.968(6)	1.961(6)	1.989(5)	1.829(4)	1.482(6)	1.554(7)	1.444(6)	1.518(7) (R = C(33)*i*-Pr)
1c	1.936(6)	1.971(6)	1.997(5)	1.824(5)	1.458(7)	1.486(8)	1.440(7)	1.893(6) (R = Br(1))

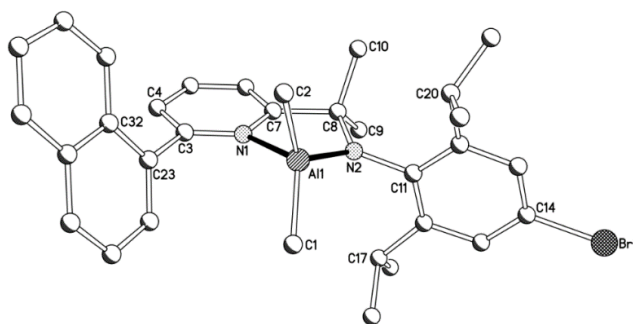| Complex	Bond Angles (deg)						
	C(1)–Al(1)–C(2)	C(1)–Al(1)–N(1)	C(1)–Al(1)–N(2)	C(2)–Al(1)–N(1)	C(2)–Al(1)–N(2)	N(1)–Al(1)–N(2)	C(7)–C(8)–N(2)
1a	113.55(11)	119.55(10)	117.79(10)	98.75(10)	118.79(10)	83.40(8)	106.31(17)
1b	111.1(3)	114.3(2)	117.5(2)	106.3(2)	119.0(3)	85.4(2)	107.9(4)
1c	113.5(3)	119.9(3)	113.4(3)	101.3(2)	121.3(2)	83.9(2)	107.0(5)

Figure 3. Molecular structure of **1c** with atom labeling scheme. All hydrogen atoms have been omitted for clarity.

Support for the solid state structures of **1a–1c** being maintained in solution is provided by the inequivalency of the backbone N-CMe[A]Me[B] methyl protons in their ^{1}H NMR spectra (recorded in C_6D_6 at ambient temperature), which is accompanied by two distinct septets for the Ar-*o*-C*H*Me2 protons and four separate doublets for the Ar-CH*Me*2 protons (see Figures 4, S12–S14). This inequivalency can be attributed to the restricted rotation of the naphthyl group; for purposes of comparison the ^{1}H NMR spectra of [2-{CMe2N(2,6-*i*-Pr2C6H3)}-6-(R)C5H3N]AlMe2 (R = H, *i*-Pr, *t*-Bu) show the corresponding NCMe2 and Ar-*o*-C*H*Me2 protons to be in equivalent environments [45]. The restricted rotation of the naphthyl group in **1a–1c** also has the effect that the methyl ligands occupy distinct environments with two well separated signals seen upfield (at *ca.* δ −0.24 and δ−1.15); this is further mirrored in the ^{13}C{^{1}H} NMR spectra with the corresponding methyl carbon resonances occurring as two quadrupolar broadened peaks between δ −5.5 and −9.4 (Figures S15–S17). No additional information regarding the barrier to rotation could be obtained on recording the ^{1}H NMR spectrum of **1a** at higher temperature. The FAB mass spectra (using nitrophenyloctylether as the matrix) of **1a–1c** show weak molecular ion peaks along with more intense fragmentation peaks corresponding to the loss of a methyl in each case. Microanalytical data further support the composition of the complexes.
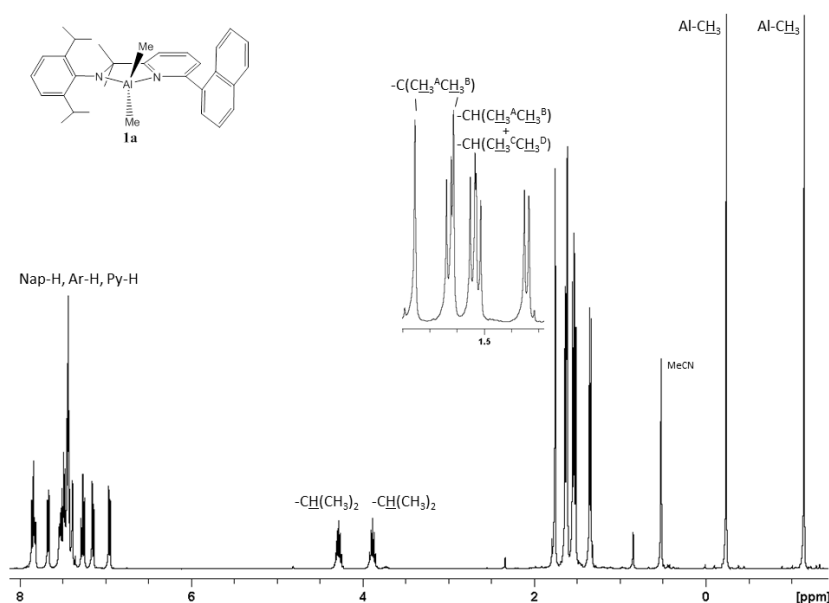

Figure 4. ^{1}H NMR (400 MHz) spectrum of **1a** in C_6D_6 at room temperature.

2.2. Polymerization Results

Complexes **1a**–**1c** were all screened as pro-initiators for the ring-opening polymerization of ε-CL. Typically, **1a**–**1c** were treated with one equivalent of benzyl alcohol in toluene prior to the addition of the ε-CL (250 equivalents) and the start of the run; all systems were evaluated at 30 °C and selected examples at 50 °C (Scheme 2). The polymerization runs were monitored at 30 min intervals by ^{1}H NMR spectroscopy to determine the ε-CL to poly(CL) conversion. In addition the resultant polycaprolactone polymers were analyzed by size exclusion chromatography (SEC).
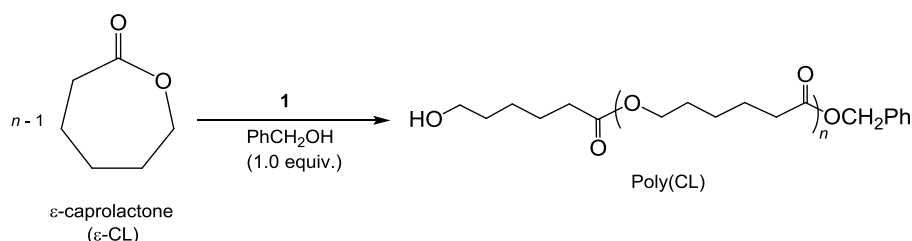
Scheme 2. Catalytic evaluation of **1**/PhCH$_2$OH for the ROP of ε-CL.

The results of the catalytic screening are collected in Table 3 (entries 1–14). At 30 °C, all the systems display moderate to good activity [5] for the polymerization of ε-CL with *para-i*-Pr-containing **1b**/PhCH$_2$OH being the most active reaching 80% conversion to poly(CL) after 2 h (entry 8). The *para*-Br-containing **1c**/PhCH$_2$OH and *para*-H-containing **1a**/PhCH$_2$OH proved less active reaching only 38% (entry 12) and 59% (entry 4) over the same time period, respectively. In the case of **1b**, full conversion was reached after only one hour when the run was performed at 50 °C (entry 14).

Table 3. Ring opening polymerization of ε-CL initiated by **1**/PhCH$_2$OH catalyst systems [a].

Entry	Pro-Initiator (R)	Temp./°C	Time/min	Conversion/% [b]	M_n (SEC) [c]	M_n (Calcd) [d]	Đ
1	**1a** (H)	30	30	18	6750	5340	1.33
2	**1a** (H)	30	60	36	12180	10370	1.58
3	**1a** (H)	30	90	40	11740	11510	1.57
4	**1a** (H)	30	120	59	19010	16920	1.38
5	**1b** (*i*-Pr)	30	30	35	8700	9990	1.47
6	**1b** (*i*-Pr)	30	60	60	16540	17210	1.39
7	**1b** (*i*-Pr)	30	90	73	18850	20910	1.46
8	**1b** (*i*-Pr)	30	120	80	20790	22910	1.39
9	**1c** (Br)	30	30	13	4250	3810	1.14
10	**1c** (Br)	30	60	25	8270	7230	1.14
11	**1c** (Br)	30	90	34	11060	9800	1.09
12	**1c** (Br)	30	120	38	10810	10940	1.24
13	**1b** (*i*-Pr)	50	30	86	20270	24620	1.65
14	**1b** (*i*-Pr)	50	60	100	28880	28610	1.61

[a] Conditions: **1** (0.04 mmol), PhCH$_2$OH (0.04 mmol), ε-CL (10 mmol) ([CL]/[Al] = 250), toluene at the given temperature; [b] Estimated by ^{1}H NMR spectroscopy; [c] By size exclusion chromatography (SEC) in THF *vs.* polystyrene standards, values corrected according to the equation $M_{n(PCL)} = 0.56 \times M_{n(SEC\ vs\ polystyrene\ standards)}$ [65,66]; [d] Calculated from [the molecular weight of ε-CL × [CL]/[Al] × the conversion] + the molecular weight of benzyl alcohol.

The dispersities of the polyesters were narrow with unimodal characteristics ($Đ = M_w/M_n = 1.09$ to 1.65) with the runs for **1b** performed at the higher temperatures (entries 13,14) falling at the higher end of the range. All three systems display an approximately linear relationship between number-average molecular weight (M_n) and monomer conversion which, coupled with the relatively low values of the dispersities, implies controlled polymerizations (Figure 5). The apparent broadening of the dispersities at higher temperature would suggest the onset of some transesterification reactions albeit minimal.
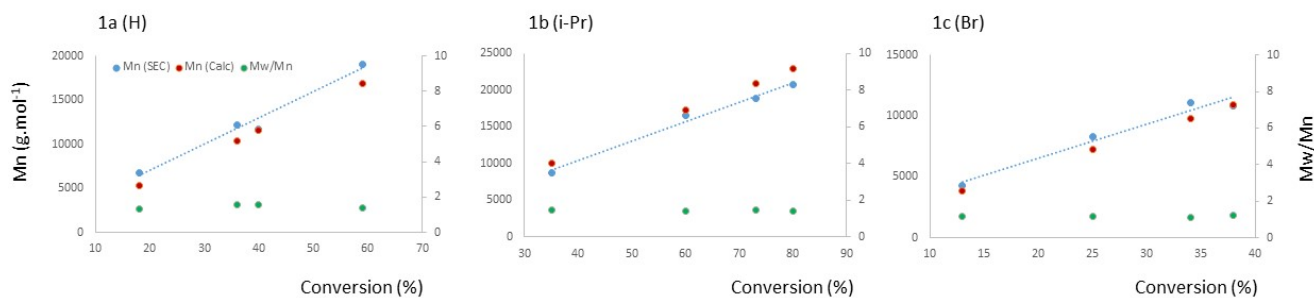

Figure 5. Number-average molar mass (M_n) and dispersity ($M_w/M_n = Đ$ *vs.* conversion for samples **1a** (H), **1b** (*i*-Pr) and **1c** (Br). Dotted blue (M_n obtained by SEC), dotted red (M_n calculated), dotted green (M_w/M_n obtained by SEC).

In general, there was reasonable agreement between the observed and calculated molecular weights, again indicating good control over the polymerization process. The MALDI-ToF spectrum of a sample of PCL obtained from **1a**/PhCH$_2$OH reveals a series of major peaks separated by a caprolactone unit (114 g·mol^{-1}) corresponding to linear [H–(CL)$_n$–OBn]·Na$^+$ cations (see Figure S18). This would suggest a coordination-insertion mechanism, as seen by others, is operational making use of an Al-OCH$_2$Ph group in the polymerization [1–5]. Moreover, the ^{1}H NMR spectrum of a sample of PCL obtained using the same catalyst showed a peak at 5.12 ppm corresponding to the benzyl ester end group and a signal at 3.65 ppm to the hydroxymethylene (–CH$_2$OH) end group. Unexpectedly, the same MALDI-ToF spectrum also displayed minor peaks that could be assigned to linear [H–(CL)$_n$–OH]·Na$^+$ cations, the likely product of hydrolysis under ionization conditions.

It is apparent from the above results that the electron-donating capacity of the *N*-aryl 4-R group of the *N,N*-pyridine-alkylamide ancillary ligand influences the catalytic activity with *para*-isopropyl-containing **1b** showing the highest activity; unexpectedly, however, the more electron-withdrawing *para*-bromo **1c** is more active than the *para*-hydrogen **1a**. It has been proposed previously that the overall rate of the polymerization depends on a combination of factors including the Lewis acidity of the metal center and the alkoxide nucleophilicity [17]. For the systems described in this work it would appear that there is a delicate balance between these factors with the superior alkoxide nucleophilicity in **1b**/PhCH$_2$OH likely to more influential in this case; similar electron donating rate enhancements have been noted elsewhere [17,32,67]. Undoubtedly the rearrangements that ensue in the final ring opening of the monomer further contribute to the overall polymerization rate.

Given the inequivalence of the aluminum methyl ligands of **1a**–**1c** in the ^{1}H NMR spectra (*vide supra*), it was of interest to monitor any site selectivity in the reaction with benzyl alcohol. Unfortunately, on treatment of **1a** with one equivalent of benzyl alcohol in C$_6$D$_6$ a mixture of products

was formed as evidenced by a series of the peaks in ^{1}H NMR spectrum in the region characteristic of the Al–OCH2Ph protons (between δ 4.9–5.4) [19,68]. This observation would suggest that the presence of ε-CL is crucial for generating the single active Al-benzyloxide species.

3. Experimental Section

3.1. General Procedures

All reactions, unless otherwise stated, were carried out under an atmosphere of dry, oxygen-free nitrogen, using standard Schlenk techniques. Solvents were distilled under nitrogen from appropriate drying agents and degassed prior to use [69]. NMR spectra were recorded on a Bruker DRX400 spectrometer (Coventry, UK) at 400.13 (^{1}H) and 100.61 MHz (^{13}C) at ambient temperature unless otherwise stated; chemical shifts (ppm) are referred to the residual protic solvent peaks and coupling constants are expressed in hertz (Hz). The electrospray ionization (ESI) and the fast atom bombardment (FAB) mass spectra were recorded using a micromass Quattro LC mass spectrometer (Manchester, UK) and a Kratos Concept spectrometer (Manchester, UK) with methanol or nitrophenyloctylether as the matrix, respectively. High-resolution FAB mass spectra were recorded on Kratos Concept spectrometer (xenon gas, 7 kV) with NBA as matrix. The MALDI-ToF mass spectrum of PCL was obtained with an ABI Voyager-DE™ STR (Warrington, UK), BioSpectrometry™ Workstation (Warrington, UK), Serial No.: 4364, using a nitrogen laser source (337 nm, delay time 500 ns) in reflector mode with a positive acceleration voltage of 25 kV. The infrared spectra were recorded on a Perkin-Elmer Spectrum One FT-IR spectrometer (Buckinghamshire, UK) on solid samples. Melting points (mp) were measured on a Gallenkamp melting point apparatus (model MFB-595, Loughborough, UK) in open capillary tubes and were uncorrected. Elemental analyses were performed on a Carlo Erba CE1108 instrument at the Department of Chemistry, London Metropolitan University (London, UK).

The reagents, 2,6-diisopropylaniline, and trimethylaluminum (2M solution in toluene) were purchased from Sigma-Aldrich Company Ltd. (Dorset, England) and used without further purification. Both benzyl alcohol and ε-caprolactone were purchased from Aldrich and distilled prior to use. The compounds 2,4,6-triisopropylaniline [70], 4-bromo-2,6-diisopropylaniline [71], 1-naphthyl boronic acid [72], 2-bromo-6-acetylpyridine [73], and tetrakis(triphenylphosphine)palladium(0) [74], were prepared according to previously reported procedures. All other chemicals were obtained commercially and used without further purification.

3.2. Synthesis of 2-{CMe=O}-6-(1-C10H7)C5H3N

The title compound was prepared using a modification of a previously reported procedure [61]. A flask was charged with 2-bromo-6-acetylpyridine (1.788 g, 8.94 mmol), tetrakis(triphenylphosphine) palladium(0) (0.207 g, 0.179 mmol, 2 mol %), 2M aqueous potassium carbonate (8.94 mL, 17.88 mmol, 2 eq.), and toluene (30 mL). The mixture was stirred for 20 min at room temperature followed by the addition of 1-naphthyl boronic acid (2.00 g, 11.62 mmol, 1.3 eq.) and ethanol (10 mL). After stirring the reaction mixture at 90 °C for 72 h, the flask was allowed to cool to room temperature, 30% hydrogen peroxide (0.7 mL) cautiously added, and the solution stirred for 1 h. The organic phase

was separated and the aqueous phase washed with chloroform (3 × 50 mL). The combined organic phases were washed with brine (1 × 30 mL), dried over $MgSO_4$, filtered, and the solvent removed under reduced pressure. The resulting oil was subject to flash-column silica chromatography employing dichloromethane/petroleum ether as the eluent (3:1). After removing the solvent under reduced pressure 2-(1-naphthyl)-6-acetylpyridine was obtained as a yellow solid (2.19 g, 99%). ^1H NMR (400 MHz, $CDCl_3$): δ 2.76 (s, 3H, O=CCH$_3$), 7.48–7.55 (m, 2H, Ar–H), 7.58 (t, *J* 7.6, 1H, Py–H), 7.66 (dd, *J* 7.1, 1.4, 1H, Py–H/Nap–H), 7.78 (dd, *J* 7.7, 1.1, 1H, Py–H/Nap–H), 7.93–7.98 (m, 3H, Nap–H), 8.09 (dd, *J* 7.8, 1.1, 1H, Nap–H), 8.17 (dd, *J* 8.1, 1.0, 1H, Nap–H). ESI MS: *m/z* 248 [M + H]$^+$, 270 [M + Na]$^+$. The ^1H NMR data were consistent with that described in the literature [61].

3.3. Synthesis of 2-{CMe=N(Ar)}-6-(1-C$_{10}$H$_7$)C$_5$H$_3$N

3.3.1. Ar = 2,6-*i*-Pr$_2$C$_6$H$_3$ (**L1**$_{dipp}$)

A round bottomed flask equipped with stir bar and reflux condenser was charged with 2-(1-naphthyl)-6-acetylpyridine (0.538 g, 2.18 mmol), methanol (4 mL), and 2,6-diisopropylaniline (0.579 g, 3.27 mmol, 1.5 eq). The reaction mixture was stirred and heated to reflux and, after 15 min, 2 drops of formic acid added. The reaction was left to stir at reflux for a further 3 days. On cooling to room temperature, the reaction mixture was left to stand for 3 h. The resulting yellow precipitate was filtered, washed with cold methanol and dried under reduced pressure to give **L1**$_{dipp}$ as a yellow solid (0.587 g, 66%). M.p. 180–181 °C. ^1H NMR (400 MHz, $CDCl_3$): δ 1.16 (d, *J* 7.0, 6H, CH(CH$_3$)$_2$), 1.19 (d, *J* 6.8, 6H, CH(CH$_3$)$_2$), 2.26 (s, 3H, N=CCH$_3$), 2.82 (sept, *J* 7.2, 2H, CH(CH$_3$)$_2$), 7.09 (dd, *J* 8.5, 6.7, 1H, dipp-H), 7.17 (d, *J* 7.0, 2H, dipp-H), 7.46–7.49 (m, 2H, Nap–H), 7.58 (dd, *J* 8.2, 7.2, 1H, Py–H), 7.67–7.71 (m, 2H, Py–H/Nap–H), 7.90–7.94 (m, 3H, Nap–H), 8.28–8.30 (m, 1H, Nap–H), 8.40 (dd, *J* 7.9, 0.9, 1H, Nap–H). ^{13}C{^1H} NMR (100 MHz, $CDCl_3$): δ 16.4 (CH$_3$), 21.9 (2CH$_3$), 22.3 (2CH$_3$), 27.3 (2CH), 118.4, 122.0, 122.5, 124.3, 124.7, 124.9, 125.0, 125.4, 126.8, 127.4, 128.1 (CH), 130.2, 133.1, 134.8 (C), 135.8 (CH), 137.3, 145.6, 155.2, 157.0 (C), 166.4 (C=N$_{imine}$). IR ν$_{max}$ (solid)/cm^{-1} 1638 (C=N$_{imine}$), 1570 (C=N$_{py}$). ESI MS: *m/z* 407 [M + H]$^+$. HRMS (TOF): Calcd for C$_{29}$H$_{31}$N$_2$O [M + H]$^+$: 407.2487, found: 407.2496.

3.3.2. Ar = 2,4,6-*i*-Pr$_3$C$_6$H$_2$ (**L1**$_{tripp}$)

A similar procedure to that outlined for **L1**$_{dipp}$ was followed using 2-(1-naphthyl)-6-acetylpyridine (0.538 g, 2.18 mmol), methanol (4 mL), and 2,4,6-triisopropylaniline (0.717 g, 3.27 mmol) gave **L1**$_{tripp}$ as a yellow-orange solid (0.653 g, 67%). M.p. 121–122 °C. ^1H NMR (400 MHz, $CDCl_3$): δ 1.16 (d, *J* 6.9, 6H, *ortho*-CH(CH$_3$)$_2$), 1.19 (d, *J* 6.8, 6H, *ortho*-CH(CH$_3$)$_2$), 1.29 (d, *J* 6.9, 6H, *para*-CH(CH$_3$)$_2$), 2.26 (s, 3H, N=CCH$_3$), 2.79 (sept, *J* 7.2, 2H, CH(CH$_3$)$_2$), 2.90 (sept, *J* 7.2, 1H, CH(CH$_3$)$_2$), 7.02 (s, 2H, tripp-H), 7.47–7.51 (m, 2H, Nap–H), 7.56 (dd, *J* 8.2, 7.2, 1H, Py–H), 7.66–7.70 (m, 2H, Py–H/Nap–H), 7.88–7.92 (m, 3H, Py–H/Nap–H), 8.28–8.31 (m, 1H, Nap–H), 8.40 (dd, *J* 7.9, 0.9, 1H, Nap–H). ^{13}C{^1H} NMR (100 MHz, $CDCl_3$): δ 16.4 (CH$_3$), 22.0 (2CH$_3$), 22.3 (2CH$_3$), 23.3 (2CH$_3$), 27.3 (2CH), 33.0 (CH), 118.4, 119.8, 124.3, 124.7, 124.8, 124.9, 125.3, 126.8, 127.4, 128.0 (CH), 130.2, 133.0, 134.3 (C), 135.4 (CH), 137.3, 142.5, 143.3, 155.3, 156.9 (C),

166.3 (C=N$_{imine}$). IR: ν_{max} (solid)/cm^{-1} 1638 (C=N$_{imine}$), 1570 (C=N$_{py}$). ESI MS: *m/z* 449 [M + H]$^{+}$. HRMS (TOF): Calcd for C$_{32}$H$_{37}$N$_{2}$ [M + H]$^{+}$: 449.2957, found: 449.2966.

3.3.3. Ar = 4-Br-2,6-*i*-Pr$_{2}$C$_{6}$H$_{2}$ (**L1**$_{Brdipp}$)

A similar procedure to that outlined for **L1**$_{dipp}$ was followed using 2-(1-naphthyl)-6-acetylpyridine (0.538 g, 2.18 mmol), methanol (4 mL), and 4-bromo-2,6-diisopropylaniline (0.836 g, 3.27 mmol) affording **L1**$_{Brdipp}$ as a light green solid (0.756 g, 71%). M.p. 160–162 °C. ^{1}H NMR (400 MHz, CDCl$_{3}$): δ 1.15 (t, *J* 7.0, 12H, CH(CH$_{3}$)$_{2}$), 2.25 (s, 3H, N=CCH$_{3}$), 2.77 (sept, *J* 6.8, 2H, CH(CH$_{3}$)$_{2}$), 7.27 (s, 2H, Brdipp-H), 7.49 (m, 2H, Nap–H), 7.57 (dd, *J* 8.1, 7.2, 1H, Py–H), 7.67–7.70 (m, 2H, Py–H/Nap–H), 7.90–7.94 (m, 3H, Py–H/Nap–H), 8.27 (m, 1H, Nap–H), 8.36 (dd, *J* 7.9, 0.9, 1H, Nap–H), ^{13}C{^{1}H} NMR (100 MHz, CDCl$_{3}$): δ 16.4 (CH$_{3}$), 21.6 (2CH$_{3}$), 22.1 (2CH$_{3}$), 27.4 (2CH), 115.8 (CBr), 118.4, 124.3, 124.6, 124.9, 125.2, 125.4, 126.8, 127.4, 128.1 (CH), 130.1, 133.0 (C), 135.9 (CH), 137.2, 137.3, 144.6, 154.8, 157.1 (C), 167.1 (C=N$_{imine}$). IR: ν_{max} (solid)/cm^{-1} 1646 (C=N$_{imine}$), 1568 (C=N$_{py}$). ESI MS: *m/z* 485, 487 [M + H]$^{+}$. HRMS (TOF): Calcd for C$_{29}$H$_{30}$BrN$_{2}$ [M + H]$^{+}$: 485.1592, 487.1572, found: 485.1609, 487.1600.

3.4. Synthesis of Complexes [2-{CMe$_{2}$N(Ar)}-6-(1-C$_{10}$H$_{7}$)C$_{5}$H$_{3}$N]AlMe$_{2}$ (1)

3.4.1. Ar = 2,6-*i*-Pr$_{2}$C$_{6}$H$_{3}$ (**1a**)

An oven-dried Schlenk vessel equipped with a magnetic stir bar was evacuated and backfilled with nitrogen. The vessel was charged with **L1**$_{dipp}$ (0.200 g, 0.492 mmol) and toluene (10 mL). Trimethylaluminum (0.50 mL, 0.984 mmol; 2M solution in toluene) was introduced and the reaction mixture stirred and heated to 110 °C overnight. On cooling to room temperature, all volatiles were removed under reduced pressure. Acetonitrile (15 mL) was introduced and the suspension heated until dissolution using a heat gun. The hot solution was transferred by cannular filtration into a second oven-dried Schlenk vessel. On standing at room temperature, pale yellow crystals of **1a** were obtained. The crystals were filtered and dried under reduced pressure (0.140 g, 60%). M.p. > 255 °C (decomp.). ^{1}H NMR (400 MHz, C$_{6}$D$_{6}$): δ −1.15 (s, 3H, Al–CH$_{3}$), −0.25 (s, 3H, Al–CH$_{3}$), 1.34 (d, *J* 6.7, 3H, CH(CH$_{3}$)), 1.52 (d, *J* 6.8, 3H, CH(CH$_{3}$)), 1.54 (d, *J* 6.9, 3H, CH(CH$_{3}$)), 1.61 (s, 3H, CCH$_{3}$), 1.63 (d, *J* 6.9, 3H, CH(CH$_{3}$)), 1.75 (s, 3H, CCH$_{3}$), 3.88 (sept, *J* 7.1, 1H, CH(CH$_{3}$)$_{2}$), 4.27 (sept, *J* 7.1, 1H, CH(CH$_{3}$)$_{2}$), 6.95 (dd, *J* 7.5, 0.9, 1H, Py–H), 7.14 (dd, *J* 7.7, 0.9, 1H, Py–H), 7.26 (t, *J* 6.9, 1H, Py–H), 7.41–7.50 (m, 7H, Ar–H/Nap–H), 7.66 (dd, *J* 6.5, 1.0, 1H, Ar–H/Nap–H), 7.81–7.85 (m, 2H, Ar–H/Nap–H). ^{13}C {^{1}H} NMR (100 MHz, C$_{6}$D$_{6}$): δ −9.3 (Al–C), −5.5 (Al–C), 22.8 (CH$_{3}$), 22.9 (CH$_{3}$), 26.1 (CH$_{3}$), 26.2 (CH$_{3}$), 26.7 (CH), 26.8 (CH), 28.5 (CH$_{3}$), 30.5 (CH$_{3}$), 62.3 (N–C), 118.7, 122.4, 123.1, 123.2, 123.5, 124.0, 125.1, 125.7, 127.3, 127.4, 129.2 (C–H), 131.1, 132.4, 132.9 (C), 138.1 (C–H), 142.1, 149.6, 149.7, 154.8, 172.1 (C). IR: ν_{max} (solid)/cm^{-1} 1566 (C=N$_{py}$). Microanalysis: Anal Calc. for (C$_{32}$H$_{39}$AlN$_{2}$): C, 80.33; H, 8.16; N, 5.86, found: C, 80.27; H, 8.36; N, 5.94%. FAB MS: *m/z* 479 [M]$^{+}$, 463 [M–CH$_{3}$]$^{+}$. Decomp. > 255 °C.

3.4.2. Ar = 2,4,6-*i*-Pr$_3$C$_6$H$_2$ (**1b**)

A similar procedure to that outlined for **1a** was followed using **L1**$_{tripp}$ (0.220 g, 0.492 mmol), toluene (10 mL), and trimethylaluminum (0.50 mL, 0.984 mmol; 2M solution in toluene) gave **1b** as brown crystals (0.130 g, 51%). M.p. > 255 °C (decomp.). ^{1}H NMR (400 MHz, C$_6$D$_6$):δ −1.14 (s, 3H, Al-CH$_3$), −0.25 (s, 3H, Al–CH$_3$), 1.42 (d, *J* 6.7, 3H, CH(CH$_3$)), 1.53 (d, *J* 6.9, 6H, CH(CH$_3$)), 1.60 (d, *J* 6.7, 3H, CH(CH$_3$)), 1.62 (s, 3H, C(CH$_3$), 1.63 (d, *J* 6.8, 3H, CH(CH$_3$)), 1.72 (d, *J* 6.9, 3H, CH(CH$_3$)), 1.76 (s, 3H, C(CH$_3$), 3.13 (sept, *J* 7.2, 1H, CH(CH$_3$)$_2$), 3.95 (sept, *J* 7.1, 1H, CH(CH$_3$)$_2$), 4.31 (sept, *J* 7.1, 1H, CH(CH$_3$)$_2$), 6.96 (dd, *J* 7.2, 1.0, 1H, Py–H), 7.16 (dd, *J* 8.1, 1.0, 1H, Py–H), 7.28 (t, *J* 3.9, 1H, Py–H), 7.45–7.54 (m, 6H, Ar–H/Nap–H), 7.67 (dd, *J* 7.1, 1.0, 1H, Ar–H/Nap–H), 7.82–7.86 (m, 2H, Ar–H/Nap–H). ^{13}C {^{1}H} NMR (100 MHz, C$_6$D$_6$): δ −9.2 (Al–C), −5.5 (Al–C), 22.9 (CH$_3$), 23.0 (CH$_3$), 23.1 (2CH$_3$), 26.3 (CH$_3$), 26.3 (CH$_3$), 26.8 (CH), 26.9 (CH), 28.7 (CH$_3$), 30.4 (CH$_3$), 33.0 (C–H), 62.4 (N–C), 118.8, 120.1, 120.2, 123.2, 123.5, 124.0, 125.1, 125.6, 127.4, 129.1 (C–H), 131.1, 132.4, 132.9 (C), 138.1 (CH), 139.6, 142.5, 149.2, 149.3, 154.7, 172.2 (C). IR: ν$_{max}$ (solid)/cm^{-1} 1571 (C=N$_{py}$). Microanalysis: Anal Calc. for (C$_{35}$H$_{45}$AlN$_2$): C, 80.73; H, 8.71; N, 5.38, Found: C, 80.69; H, 8.83; N, 5.56. FAB MS: *m/z* 520 [M]$^+$, 505 [M–CH$_3$]$^+$. TOF MS: Calcd for C$_{35}$H$_{45}$AlN$_2$ [M + H]$^+$: 521.3476, found: 521.3475.

3.4.3. Ar = 4-Br-2,6-*i*-Pr$_2$C$_6$H$_2$ (**1c**)

A similar procedure to that outlined for **1a** was followed using **L1**$_{Brdipp}$ (0.240 g, 0.492 mmol), toluene (10 mL), and trimethylaluminum (0.50 mL, 0.984 mmol; 2M solution in toluene) gave **1c** as pale green crystals (0.209 g, 76%). M.p. > 255 °C (decomp.). ^{1}H NMR (400 MHz, C$_6$D$_6$): δ −1.15 (s, 3H, Al–CH$_3$), −0.24 (s, 3H, Al–CH$_3$), 1.25 (d, *J* 6.7, 3H, CH(CH$_3$)), 1.43 (d, *J* 6.8, 6H, CH(CH$_3$)), 1.51 (d, *J* 6.9, 3H, CH(CH$_3$)), 1.57 (s, 3H, CCH$_3$), 1.72 (s, 3H, CCH$_3$), 3.80 (sept, *J* 7.1, 1H, CH(CH$_3$)$_2$), 4.18 (sept, *J* 1.1, 1H, CH(CH$_3$)$_2$), 6.99 (d, *J* 7.5, 1H, Py–H), 7.17 (d, *J* 8.1, 1H, Py–H), 7.32 (t, *J* 7.9, 1H, Py–H), 7.49–7.52 (m, 4H, Ar–H/Nap–H), 7.68 (d, *J* 7.0, 1H, Ar–H/Nap–H), 7.73 (d, *J* 2.5, 1H, Ar–H/Nap–H), 7.78 (d, *J* 2.5, 1H, Ar–H/Nap–H), 7.88–7.92 (m, 2H, Ar–H/Nap–H). ^{13}C {^{1}H} NMR (100 MHz, C$_6$D$_6$): δ −9.4 (Al–C), −5.6 (Al–C), 22.4 (2CH$_3$), 25.8 (2CH$_3$), 26.8 (CH), 26.9 (CH), 28.3 (CH$_3$), 30.4 (CH$_3$), 62.3 (N–C), 117.2 (C–Br), 118.6, 123.3, 123.4, 123.9, 125.2, 125.7, 125.8, 127.3, 127.5, 129.1, 129.2 (C-H), 131.0, 132.4, 132.7 (C), 138.3 (CH), 141.6, 152.5, 152.6, 154.8, 171.6 (C). IR: ν$_{max}$ (solid)/cm^{-1} 1569 (C=N$_{py}$). FABMS: *m/z* 557 [M]$^+$, 543 [M − CH$_3$]$^+$.

3.5. Procedure for ROP and SEC Details

3.5.1. Catalytic Evaluation

A typical polymerization procedure is as follows (Table 3). An oven-dried Schlenk vessel equipped with stirrer bar was loaded in the glove box. The aluminum pro-initiator **1** (0.04 mmol) was introduced, followed by 15 mL of a 0.0027 M solution of benzyl alcohol (0.04 mmol, 1 eq.) in toluene. The mixture was stirred for 10 min at room temperature and then placed in an oil bath pre-heated to the desired temperature. ε-CL (1.1 mL, 10.0 mmol, 250 eq.) was added and the mixture allowed to stir for the designated time period. A small aliquot (0.2 mL) of the reaction mixture was removed at

selected time intervals, treated with a few drops of methanol and the residue analyzed by ^{1}H NMR spectroscopy (to determine monomer conversion) and by SEC (to determine M_n and $Đ$). All conversion measurements were repeated in triplicate.

3.5.2. Size Exclusion Chromatography

Size Exclusion Chromatography analyses of the samples were performed on an EcoSEC semi-micro GPC system from Tosoh (Minato-ku, TKY, Japan) equipped with a dual flow refractive index detector and a UV detector. The samples were analyzed in THF at 30 °C using a flow rate of 1 mL·min^{-1}. All polymers were injected at a concentration of 1 mg·mL^{-1} in THF, after filtration through a 0.45 μm pore-size membrane. Separation was performed with a guard column and three PL gel 5 μm MIXED-C (7 μm, 300 × 7.5 mm). The average molar masses (number-average molar mass M_n and weight-average molar mass M_w) and the dispersity ($Đ = M_w/M_n$) were derived from the RI signal by a calibration curve based on poly (styrene) standards. The calibration was constructed with narrow molecular weight standards from 580 g/mol to 3,053,000 g/mol. A third-degree polynomial regression was applied. WinGPC software (PSS Polymer Standards Service, Mainz, Germany) was used for data collection and calculation. The M_n values of the PCLs were corrected with a factor of 0.56 to account for the difference in hydrodynamic volumes with polystyrene [65,66].

3.6. Crystallographic Studies

Data for **L1**$_{dipp}$, **L1**$_{tripp}$, **1a**, **1b** and **1c** were collected on a Bruker APEX 2000 CCD diffractometer. Details of data collection, refinement and crystal data are listed in Table 4. The data were corrected for Lorentz and polarization effects and empirical absorption corrections applied. Structure solution by direct methods and structure refinement based on full-matrix least-squares on F^2 employed SHELXTL version 6.10 [75]. Hydrogen atoms were included in calculated positions (C–H = 0.95–1.00 Å) riding on the bonded atom with isotropic displacement parameters set to 1.5 U_{eq}(C) for methyl H atoms and 1.2 U_{eq}(C) for all other H atoms. All non-H atoms were refined with anisotropic displacement parameters. Disordered solvent was omitted using the SQUEEZE option in PLATON for **1c** [76].

Table 4. Crystallographic and data processing parameters for **L1**$_{dipp}$, **L1**$_{tripp}$, **1a**, **1b** and **1c**.

Complex	L1$_{dipp}$	L1$_{tripp}$	1a	1b	1c
Formula	$C_{29}H_{30}N_2$	$C_{32}H_{36}N_2$	$C_{32}H_{39}N_2Al$	$C_{35}H_{45}N_2Al$	$C_{32}H_{40}BrN_2OAl·1.5OH_2$
M	406.55	448.63	478.63	520.71	584.56
Crystal size (mm^3)	0.26 × 0.22 × 0.19	0.42 × 0.16 × 0.04	0.40 × 0.16 × 0.12	0.21 × 0.16 × 0.15	0.16 × 0.12 × 0.05
Temperature (K)	150 (2)	150 (2)	150 (2)	150 (2)	150 (2)
Crystal system	monoclinic	triclinic	triclinic	monoclinic	monoclinic
Space group	P2(1)/c	P-1	P-1	P2 (1)/n	P2 (1)/c
a (Å)	11.490 (8)	8.991 (4)	10.662 (4)	12.133 (5)	10.967 (4)
b (Å)	13.214 (9)	11.022 (5)	10.809 (4)	17.302 (7)	15.832 (6)
c (Å)	15.214 (10)	13.139 (6)	13.680 (5)	14.609 (6)	16.957 (7)
$α$ (^{o})	90	95.509 (8)	95.348 (7)	90	90

Table 4. *Cont.*

Complex	L1$_{dipp}$	L1$_{tripp}$	1a	1b	1c
β (°)	95.243 (13)	98.517 (10)	104.935 (7)	91.243 (9)	96.335 (9)
γ (°)	90	96.640 (9)	113.807 (6)	90	90
U (Å^3)	2300 (3)	1270.6 (9)	1358.5 (9)	3066 (2)	2926.3 (19)
Z	4	2	2	4	4
D_c (Mg m^{-3})	1.174	1.173	1.170	1.128	1.327
$F(000)$	872	484	516	1128	1228
μ (Mo-K$_\alpha$)(mm^{-1})	0.068	0.068	0.097	0.091	1.464
Reflections collected	16270	9445	10786	22006	21151
Independent reflections	4050	4460	5288	5402	5145
R_{int}	0.2956	0.1405	0.0603	0.2260	0.2420
Restraints/parameters	0/285	0/314	0/720	94/353	0/333
Final R indices ($I > 2\sigma(I)$)	R_1 = 0.0754 wR$_2$ = 0.1433	R_1 = 0.0738 wR$_2$ = 0.1331	R_1 = 0.0578 wR$_2$ = 0.1109	R_1 = 0.0897 wR$_2$ = 0.1838	R_1 = 0.0750 wR$_2$ = 0.1266
All data	R_1 = 0.1283 wR$_2$ = 0.1703	R_1 = 0.1990 wR$_2$ = 0.1732	R_1 = 0.0917 wR$_2$ = 0.1235	R_1 = 0.2281 wR$_2$ = 0.2226	R_1 = 0.1690 wR$_2$ = 0.1504
Goodness of fit on F^2 (all data)	0.929	0.793	0.913	0.833	0.822

Data in common: graphite-monochromated Mo-K$_\alpha$ radiation, λ = 0.71073 Å; $R_1 = \Sigma||F_o| - |F_c||/ \Sigma|F_o|$, $wR_2 = [\Sigma w(F_o^2 - F_c^2)^2/ \Sigma w(F_o^2)^2]^{1/2}$, $w^{-1} = [\sigma^2(F_o)^2 + (aP)^2]$, $P = [max(F_o^2,0) + 2(F_c^2)]/3$, where a is a constant adjusted by the program; goodness of fit = $[\Sigma(F_o^2 - F_c^2)2/(n-p)]^{1/2}$ where n is the number of reflections and p the number of parameters.

4. Conclusions

In summary, a series of sterically-hindered four-coordinate aluminum-dimethyl complexes, [2-{CMe$_2$N(Ar)}-6-(1-C$_{10}$H$_7$)C$_5$H$_3$N]AlMe$_2$ [Ar = 2,6-*i*-Pr$_2$C$_6$H$_3$ (**1a**), 2,4,6-*i*-Pr$_3$C$_6$H$_2$ (**1b**), 4-Br-2,6-*i*-Pr$_2$C$_6$H$_2$ (**1c**)], bearing bidentate 2-(amido-prop-2-yl)-6-(1-naphthyl)pyridine ligands have been synthesized and characterized on the basis of spectroscopic and analytical data. Their structures were further confirmed by single-crystal X-ray diffraction. Multinuclear NMR spectroscopy of **1** highlights the role played by the pendant naphthyl group in conferring inequivalency to the methyl ligands. The ROPs of ε-CL using **1a**–**1c**, in the presence of PhCH$_2$OH, proceeded efficiently in a controlled fashion with the propagation rates influenced by the nature of the *N*-aryl R-substituents (*viz.* **1b** > **1a** > **1c**).

Acknowledgments

Author Contributions

G.A.S. coordinated the work and wrote the manuscript. M.P, A.P.A. and Y.D.M.C. conducted the experimental work. O.B. carried out the SEC measurements and K.S. collected and solved the crystallographic data.

Conflicts of Interest

The authors declare no conflict of interest.

References

1. O'Keefe, B.J.; Hillmyer, M.A.; Tolman, W.B. Polymerization of lactide and related cyclic esters by discrete metal complexes. *Dalton Trans*. **2001**, doi:10.1039/B104197P.

2. Dechy-Cabaret, O.; Martin-Vaca, B.; Bourissou, D. Controlled ring-opening polymerization of lactide and glycolide. *Chem. Rev*. **2004**, *104*, 6147–6176.

3. Stridsberg, K.M.; Ryner M.; Albertsson, A.-C. Controlled Ring-Opening Polymerization: Polymers with designed Macromolecular Architecture. *Adv. Polym. Sci.* **2002**, *157*, 41–65.

4. Wu, J.; Yu, T.-L.; Chen, C.-T.; Lin, C.-C. Recent developments in main group metal complexes catalyzed/initiated polymerization of lactides and related cyclic esters. *Coord. Chem. Rev*. **2006**, *250*, 602–626.

5. Arbaoui, A.; Redshaw, C. Metal catalysts for ε-caprolactone polymerization. *Polym. Chem*. **2010**, *1*, 801–826.

6. Aida, T.; Inoue, S. Formation of Poly(lactide) with Controlled Molecular Weight. Polymerization of Lactide by Aluminum Porphyrin. *Chem. Lett.* **1987**, *16*, 991–994.

7. Cameron, P.A.; Jhurry, D.; Gibson, V.C.; White, A.J.P.; Williams, D.J.; Williams, S. Controlled polymerization of lactides at ambient temperature using [5-Cl-salen]AlOMe. *Macromol. Rapid Commun*. **1999**, *20*, 616–618.

8. Hormnirun, P.; Marshall, E.L.; Gibson, V.C.; White, A.J.P.; Williams, D.J. Remarkable Stereocontrol in the Polymerization of Racemic Lactide Using Aluminum Initiators Supported by Tetradentate Aminophenoxide Ligands. *J. Am. Chem. Soc*. **2004**, *126*, 2688–2689.

9. Hormnirun, P.; Marshall, E.L.; Gibson, V.C.; Pugh, R.I.; White, A.J.P. A study of ligand substituent effects on the rate and stereoselectivity of lactide polymerization using aluminum salen-type initiators. *Proc. Natl. Acad. Sci. USA* **2006**, *103*, 15343–15348.

10. Spassky, N.; Wisniewski, M.; Pluta, C.; le Borgne, A. Highly stereoelective polymerization of *rac*-(D,L)-lactide with a Chiral Schiff's base/aluminium alkoxide initiator. *Macromol. Chem. Phys*. **1996**, *197*, 2627–2637.

11. Ovitt, T.M.; Coates, G.W. Stereoselective Ring-Opening Polymerization of meso-Lactide: Synthesis of Syndiotactic Poly (lactic acid). *J. Am. Chem. Soc*. **1999**, *121*, 4072–4073.

12. Ovitt, T.M.; Coates, G.W. Stereoselective Ring-Opening Polymerization of rac-Lactide with a Single-Site, Racemic Aluminum Alkoxide Catalyst: Synthesis of Stereoblock Poly (lactic acid). *J. Polym. Sci. Polym. Chem*. **2000**, *38*, 4686–4692.

13. Radano, C.P.; Baker, G.L.; Smith, M.R., III. Stereoselective Polymerization of a Racemic Monomer with a Racemic Catalyst: Direct Preparation of the Polylactic Acid Stereocomplex from Racemic Lactide. *J. Am. Chem. Soc*. **2000**, *122*, 1552–1553.

14. Zhong, Z.; Dijkstra, P.J.; Feijen, J. [(salen)Al]-Mediated, Controlled and Stereoselective Ring-Opening Polymerization of Lactide in Solution and without Solvent: Synthesis of Highly Isotactic Polylactide Stereocopolymers from Racemic D,L-Lactide. *Angew. Chem. Int*. **2002**, *41*, 4510–4513.

15. Nomura, N.; Ishii, R.; Akakura, M.; Aoi, K. Stereoselective ring-opening polymerization of racemic lactide using aluminum-achiral ligand complexes: Exploration of a chain-end control mechanism. *J. Am. Chem. Soc.* **2002**, *124*, 5938–5939.

16. Du, H.; Pang, X.; Yu, H.; Zhang, X.; Chen, X.; Cui, D.; Wang, X.; Jing, X. Polymerization of *rac*-Lactide Using Schiff Base Aluminum Catalysts: Structure, Activity, and Stereoselectivity. *Macromolecules* **2007**, *40*, 1904–1913.

17. Alcazar-Roman, L.M.; O'Keefe, B.J.; Hillmyer, M.A.; Tolman, W.B. Electronic influence of ligand substituents on the rate of polymerization of ε-caprolactone by single-site aluminium alkoxide catalysts. *Dalton Trans.* **2003**, doi:10.1039/B303760F.

18. Amgoune, A.; Lavanant, L.; Thomas, C.M.; Chi, Y.; Welter, R.; Dagorne, S.; Carpentier, J.-F. An Aluminum Complex Supported by a Fluorous Diamino-Dialkoxide Ligand for the Highly Productive Ring-Opening Polymerization of ε-Caprolactone. *Organometallics* **2005**, *24*, 6279–6282.

19. Chen, C.-T.; Huang, C.-A.; Huang, B.-H. Aluminium metal complexes supported by amine bis-phenolate ligands as catalysts for ring-opening polymerization of ε-caprolactone. *Dalton Trans.* **2003**, doi:10.1039/B307365C.

20. Shen, M.; Zhang, W.; Nomura, K.; Sun, W.-H. Synthesis and characterization of organoaluminum compounds containing quinolin-8-amine derivatives and their catalytic behaviour for ring-opening polymerization of ε-caprolactone. *Dalton Trans.* **2009**, doi:10.1039/B910155A.

21. Lewinski, J.; Horeglad, P.; Dranka, M.; Justyniak, I. Simple Generation of Cationic Aluminum Alkyls and Alkoxides Based on the Pendant Arm Tridentate Schiff Base. *Inorg. Chem.* **2004**, *43*, 5789–5791.

22. Ma, W.-A.; Wang, Z.-X. Zinc and Aluminum Complexes Supported by Quinoline-Based *N,N,N*-Chelate Ligands: Synthesis, Characterization, and Catalysis in the Ring-Opening Polymerization of ε-Caprolactone and *rac*-Lactide. *Organometallics* **2011**, *30*, 4364–4373.

23. Peng, K.-F.; Chen, C.-T. Synthesis and catalytic application of aluminium anilido-pyrazolate complexes. *Dalton Trans.* **2009**, doi:10.1039/b905394h.

24. Bakthavachalam, K.; Reddy, N.D. Synthesis of Aluminum Complexes of Triaza Framework Ligands and Their Catalytic Activity toward Polymerization of ε-Caprolactone. *Organometallics* **2013**, *32*, 3174–3184.

25. Gao, W.; Zhang, J.; Luo, X.; Liu, X.; Mu, Y. Al and Zn complexes bearing *N,N,N*-tridentate quinolinyl anilido-imine ligands: Synthesis, characterization and catalysis in ʟ-lactide polymerization. *Dalton Trans.* **2012**, *41*, 11454–11463.

26. Sun, W.-H; Shen, M.; Zhang, W.; Huang, W.; Liu, S.; Redshaw, C. Methylaluminium 8-quinolinolates: Synthesis, characterization and use in ring-opening polymerization (ROP) of ε-caprolactone. *Dalton Trans.* **2011**, *40*, 2645–2653.

27. Ma, W.-A.; Wang, Z.-X. Synthesis and characterisation of aluminium (III) and tin (II) complexes bearing quinoline-based *N,N,O*-tridentate ligands and their catalysis in the ring-opening polymerisation of ε-caprolactone. *Dalton Trans.* **2011**, *40*, 1778–1786.

28. Kong, W.-L.; Chaia, Z.-Y.; Wang, Z.-X. Synthesis of *N,N,O*-chelate zinc and aluminum complexes and their catalysis in the ring-opening polymerization of ε-caprolactone and *rac*-lactide. *Dalton Trans.* **2014**, *43*, 14470–14480.

29. Normand, M.; Dorcet, V.; Kirillov, E.; Capentier, J.-F. {Phenoxy-imine} aluminum *vs.* -indium Complexes for the Immortal ROP of Lactide: Different Stereocontrol, Different Mechanisms. *Organometallics* **2013**, *32*, 1694–1709.

30. Gong, S.; Ma, H. β-Diketiminate aluminium complexes: Synthesis, characterization and ring-opening polymerization of cyclic esters. *Dalton Trans.* **2008**, doi:10.1039/b802638f.

31. Yao, W.; Mu, Y.; Gao, A.; Su, Q.; Liu, Y.; Zhang, Y. Efficient ring-opening polymerization of ε-caprolactone using anilido-imine-aluminum complexes in the presence of benzyl alcohol. *Polymer* **2008**, *49*, 2486–2491.

32. Zhang, W.; Wang, Y.; Cao, J.; Wang, L.; Redshaw, C.; Sun, W.-H. Synthesis and Characterization of Dialkylaluminum Amidates and Their Ring-Opening Polymerization of ε-Caprolactone. *Organometallics* **2011**, *30*, 6253–6261.

33. Shen, M.; Huang, W.; Zhang, W.; Hao, X.; Sun, W.-H.; Redshaw, C. Synthesis and characterisation of alkylaluminium benzimidazolates and their use in the ring-opening polymerisation of ε-caprolactone. *Dalton Trans.* **2010**, *39*, 9912–9922.

34. Kampova, H.; Riemlova, E.; Klikarova, J.; Pejchal, V.; Merna, J.; Vlasak, P.S.; Svec, P.; Ruzickova, Z.; Ruzicka, A. Aluminium complexes containing *N,N'*-chelating amino-amide hybrid ligands applicable for preparation of biodegradable polymers. *J. Organomet. Chem.* **2015**, *778*, 35–41.

35. Iwasa, N.; Katao, S.; Liu, J.; Fujiki, M.; Furukawa, Y.; Nomura, K. Notable Effect of Fluoro Substituents in the Imino Group in Ring-Opening Polymerization of ε-Caprolactone by Al Complexes Containing Phenoxyimine Ligands. *Organometallics* **2009**, *28*, 2179–2187.

36. Liu, J.; Iwasa, N.; Nomura, K. Synthesis of Al complexes containing phenoxy-imine and their use as the precursors for efficient living of ε-caprolactone. *Dalton Trans.* **2008**, doi:10.1039/B801561A.

37. Tseng, H.-T., Chiang, M.Y.; Lu, W.-Y.; Chen, Y.-J.; Lian, C.-J.; Chen, Y.-H.; Tsai, H.-Y.; Lai, Y.-C.; Chen, H.-Y. A closer look at ε-caprolactone polymerization catalyzed by alkyl aluminum complexes: The effect of induction period on overall catalytic activity. *Dalton Trans.* **2015**, *44*, 11763–11773.

38. Yu, R.-C.; Huang, C.-H.; Huang, J.-H.; Lee, H.-Y.; Chen, J.-T. Four- and Five-Coordinate Aluminum Ketiminate Complexes: Synthesis, Characterization, and Ring-Opening Polymerization. *Inorg. Chem.* **2002**, *41*, 6450–6455.

39. Nomura, N.; Aoyama, T.; Ishii, R.; Kondo, T. Salicylaldimine-Aluminum Complexes for the Facile and Efficient Ring-Opening Polymerization of ε-Caprolactone. *Macromolecules* **2005**, *38*, 5363–5366.

40. Bouyayi, M.; Roisnel, T.; Carpentier, J.-F. Aluminum Complexes of Bidentate Fluorinated Alkoxy-Imino Ligands: Syntheses, Structures, and Use in Ring-Opening Polymerization of Cyclic Esters. *Organometallics* **2012**, *31*, 1458–1466.

41. Chapurina, Y.; Roisnel, T.; Carpentier, J.-F.; Kirillov, E. Zinc, aluminum and group 3 metal complexes of sterically demanding naphthoxy-pyridine ligands: Synthesis, structure, and use in ROP of racemic lactide and β-butyrolactone. *Inorg. Chim. Acta* **2015**, *431*, 161–175.

42. Li, Y.; Zhao, K.-Q.; Elsegood, M.R.J.; Prior, T.J.; Sun, X.; Mo, S.; Redshaw C. Organoaluminium complexes of *ortho*-, *meta*-, *para*-anisidines: Synthesis, structural studies and ROP of ɛ-caprolactone (and *rac*-lactide). *Catal. Sci. Technol.* **2014**, *4*, 3025–3031.

43. Myers, T.W.; Berben, L.A. A sterically demanding iminopyridine ligand affords redox-active complexes of aluminum(III) and gallium(III). *Inorg. Chem.* **2012**, *51*, 1480–1488.

44. Budzelaar, P.H.M. Radical Chemistry of Iminepyridine Ligands. *Eur. J. Inorg. Chem.* **2012**, *2012*, 530–534.

45. Nienkemper, K.; Kehr, G.; Kehr, S.; Froehlich, R.; Erker, G. (Amidomethyl) pyridine zirconium and hafnium complexes: Synthesis and structural characterization *J. Organomet. Chem.* **2008**, *693*, 1572–1589.

46. Gibson, V.C.; Redshaw, C.; White, A.J.P.; Williams, D.J. Synthesis and structural characterisation of aluminium imino-amide and pyridyl-amide complexes: Bulky monoanionic *N,N* chelate ligands via methyl group transfer. *J. Organomet. Chem.* **1998**, *550*, 453–456.

47. Wei, Y.; Wang, S.; Zhou, S.; Feng, Z.; Guo, L.; Zhu, X.; Mu, X.; Yao, F. Aluminum Alkyl Complexes Supported by Bidentate *N,N* Ligands: Synthesis, Structure, and Catalytic Activity for Guanylation of Amines. *Organometallics* **2015**, *34*, 1882–1889.

48. Bruce, M.; Gibson, V.C.; Redshaw, C.; Solan, G.A.; White, A.J.P.; Williams, D.J. Cationic alkyl aluminium ethylene polymerization catalysts based on monoanionic *N,N,N*-pyridyliminoamide ligands. *Chem. Commun.* **1998**, doi:10.1039/A807950A.

49. Arbaoui, A.; Redshaw, C.; Hughes, D.L. Multinuclear alkylaluminium macrocyclic Schiff base complexes: Influence of procatalyst structure on the ring opening polymerisation of ɛ-caprolactone. *Chem. Commun.* **2008**, doi:10.1039/B810417D.

50. Arbaoui, A.; Redshaw, C.; Hughes, D.L. One-pot conversion of tetraiminodiphenols to diiminodiaminodiphenols via methyl transfer at aluminium. *Supramol. Chem.* **2009**, *21*, 35–43.

51. Knijnenburg, Q.; Smits, J.M.M.; Budzelaar, P.H.M. Reaction of the Diimine Pyridine Ligand with Aluminum Alkyls: An Unexpectedly Complex Reaction. *Organometallics* **2006**, *25*, 1036–1046.

52. Davies, C.J.; Gregory, A.; Griffith, P.; Perkins, T.; Singh, K.; Solan, G.A. Use of Suzuki cross-coupling as a route to 2-phenoxy-6-iminopyridines and chiral 2-phenoxy-6-(methanamino) pyridines. *Tetrahedron* **2008**, *64*, 9857–9864.

53. Cross, W.B.; Hope, E.G.; Lin, Y.-H.; Macgregor, S.A.; Singh, K.; Solan, G.A.; Yahya, N. *N,N*-Chelate-control on the regioselectivity in acetate-assisted C–H activation. *Chem. Commun.* **2013**, *49*, 1918–1920.

54. Bianchini, C.; Lenoble, G.; Oberhauser, W.; Parisel, S.; Zanobini, F. Synthesis, Characterization, and Reactivity of Neutral and Cationic Pd–C,N,N Pincer Complexes. *Eur. J. Inorg. Chem.* **2005**, *2005*, 4794–4800.

55. Annunziata, L.; Pragliola, S.; Pappalardo, D.; Tedesco, C.; Pellecchia, C. New (Anilidomethyl)pyridine Titanium(IV) and Zirconium(IV) Catalyst Precursors for the Highly Chemo- and Stereoselective *cis*-1,4-Polymerization of 1,3-Butadiene. *Macromolecules* **2011**, *44*, 1934–1941.

56. Annunziata, L.; Pappalardo, D.; Tedesco, C.; Pellecchia, C. Bis[(amidomethyl)pyridine] Zirconium(IV) Complexes: Synthesis, Characterization, and Activity as Olefin Polymerization Catalysts. *Organometallics* **2009**, *28*, 688–697.

57. Frazier, K.A.; Froese, R.D.; He, Y.; Klosin, J.; Theriault, C.N.; Vosejpka, P.C.; Zhou, Z.; Abboud, K.A. Pyridylamido Hafnium and Zirconium Complexes: Synthesis, Dynamic Behavior, and Ethylene/1-Octene and Propylene Polymerization Reactions. *Organometallics* **2011**, *30*, 3318–3329.

58. Zuccaccia, C.; Macchioni, A.; Busico, V.; Cipullo, R.; Talarico, G.; Alfano, F.; Boone, H.W.; Frazier, K.A.; Hustad, P.D.; Stevens, J.C.; Vosejpka, P.C.; Abboud, K.A. Intra- and Intermolecular NMR Studies on the Activation of Arylcyclometallated Hafnium Pyridyl-Amido Olefin Polymerization Precatalysts. *J. Am. Chem. Soc*. **2008**, *130*, 10354–10368.

59. Luconi, L.; Rossin, A.; Tuci, G.; Tritto, I.; Boggioni, L.; Klosin, J.J.; Theriault, C.N.; Giambastiani, G. Facing Unexpected Reactivity Paths with ZrIV-Pyridylamido Polymerization Catalysts. *Chem.-Eur. J.* **2012**, *18*, 671–687

60. Domski, G.J.; Edson, J.B.; Keresztes, I.; Lobkovsky, E.B.; Coates, G.W. Synthesis of a new olefin polymerization catalyst supported by an sp^3-C donor via insertion of a ligand-appended alkene into the Hf–C bond of a neutral pyridylamidohafnium trimethyl complex. *Chem. Commun*. **2008**, doi:10.1039/B811384J.

61. Zhou, Y.; Kijima, T.; Izumi, T. The synthesis and application of 2-acetyl-6-(1-naphthyl)-pyridine oxime as a new ligand for palladium precatalyst in Suzuki coupling reaction. *J. Heterocycl. Chem*. **2009**, *46*, 116–118.

62. Coates, G.W.; Domski, G.J. Pyridlyamidohafnium catalyst precursors, active species from this and uses thereof to polymerize alkenes. WO 2008112133 A2, 7 March 2008.

63. Patel, P.; Chang, S. *N*-Substituted hydroxylamines as synthetically versatile amino sources in the iridium-catalyzed mild C–H amidation reaction. *Org. Lett*. **2014**, *16*, 3328–3331.

64. Kakiuchi, F.; Kochi, T.; Mutsutani, H.; Kibbayashi, N.; Urano, S.; Sato, M.; Nishiyamo, S.; Tanabe, T. Palladium-Catalyzed Aromatic C–H Halogenation with Hydrogen Halides by Means of Electrochemical Oxidation. *J. Am. Chem. Soc*. **2009**, *131*, 11310–11311.

65. Saver, M.; Schappacher, M.; Soum, A. Controlled Ring-Opening Polymerization of Lactones and Lactides Initiated by Lanthanum Isopropoxide, 1. General Aspects and Kinetics. *Macromol. Chem. Phys*. **2002**, *203*, 889–899.

66. Duda, A.; Kowalski, A.; Penczek, S. Polymerization of l,l-Lactide Initiated by Aluminum Isopropoxide Trimer or Tetramer. *Macromolecules* **1998**, *31*, 2114–2122.

67. Alkarekshi, W.; Armitage, A.P.; Boyron, O.; Davies, C.J.; Govere, M.; Gregory, A.; Singh, K.; Solan, G.A. Phenolate Substituent Effects on Ring-Opening Polymerization of ε-Caprolactone by Aluminum Complexes Bearing 2- (Phenyl-2-olate)-6-(1-amidoalkyl)pyridine Pincers. *Organometallics* **2013**, *32*, 249–259.

68. Nomura, N.; Ishii, R.; Yamamoto, Y.; Kondo, T. Stereoselective Ring-Opening Polymerization of a Racemic Lactide by Using Achiral Salen- and Homosalen-Aluminum Complexes. *Chem. Eur. J.* **2007**, *13*, 4433–4451.

69. Armarego, W.L.F.; Perrin, D.D. *Purification of Laboratory Chemicals*, 4th ed.; Butterworth Heinemann: Oxford, UK, 1996.

70. Grubert, L.; Jacobi, D.; Buck, K.; Abraham, W.; Mügge, C.; Krause, E. Pseudorotaxanes and Rotaxanes Incorporating Cycloheptatrienyl Stations—Synthesis and Co-Conformation. *Eur. J. Org. Chem*. **2001**, *2001*, 3921–3932.

71. Oskam, J.H.; Fox, H.H.; Yap, K.B.; McConville, D.H.; Odell, R.; Lichtenstein, B.J.; Schrock, R.R. Ligand variation in alkylidene complexes of the type Mo(CHR)(NR′)(OR″)$_2$. *J. Organomet. Chem.* **1993**, *459*, 185–198.

72. So, C.M.; Lau, C.P.; Chan, A.S.C.; Kwong, F.Y. Suzuki-Miyaura Coupling of Aryl Tosylates Catalyzed by an Array of Indolyl Phosphine-Palladium Catalysts. *J. Org. Chem.* **2008**, *73*, 7731–7734.

73. Parks, J.E.; Wagner, B.E.; Holm, R.H. Syntheses employing pyridyllithium reagents: New routes to 2,6-disubstituted pyridines and 6,6′-disubstituted 2,2′-bipyridyls. *J. Organomet. Chem.* **1973**, *56*, 53–66.

74. Tellier, F.; Sauvêtre, R.; Normant, J.-F. Synthese stereospecifique de dienes fluores. *J. Organomet. Chem.* **1985**, *292*, 19–28.

75. *SHELXTL*, version 6.10; Bruker AXS, Inc.: Madison, WI, USA, 2000.

76. Spek A.L. PLATON, An Integrated Tool for the Analysis of the Results of a Single Crystal Structure Determination. *Acta Cryst. Sect. A* **1990**, *A46*, C34.